

Observations of coverage- and temperature-dependent surface structures formed upon Li deposition on Cu(110)

Shigemitsu Nakanishi, Takahiro Yumura, and Kenji Umezawa

Department of Physics, University of Osaka Prefecture, Gakuencho, Sakai 593 Osaka, Japan

Hiroshi Tochihara and Seigi Mizuno

Catalysis Research Center, Hokkaido University, Kita-ku, Sapporo 060, Japan

(Received 7 September 1993)

A systematic study of surface structures of Li-covered Cu(110) was performed by means of low-energy electron-diffraction (LEED) and Auger electron spectroscopy techniques. The experiments were carried out with increasing deposition of Li both at low temperature (90 K) and room temperature (300 K). At 90 K a series of LEED patterns, (3×1) , (2×1) , (3×1) , and successive complicated structures were observed with increasing Li coverage. The sequence of the LEED patterns was interpreted as simple overlayer structures of Li in terms of a continuous increase of the packing density of deposited Li atoms sitting in the trough along the $[1\bar{1}0]$ direction of the Cu(110) surface. Marked differences in the sequence of the LEED structures were observed for observations at 300 K; the sequence of the structures was (1×2) , (1×1) , (4×1) , (5×1) , and $(n \times 1)$ where $n < 8$ with an increase of Li coverage. The first (1×2) structure was assigned to a missing-row-type restructuring of the substrate Cu atoms. The structure models for the (4×1) , (5×1) , and so on were discussed in terms of the formation of Li-Cu surface alloys proposed previously by Tochihara and Mizuno for the Li/Cu(100) system.

I. INTRODUCTION

There have been many studies on alkali-metal adsorption on metal surfaces in conjunction with practical use relating to heterogeneous catalysts and with its fundamental interest as simple adsorption system.¹ In those works, particular interest has been focused on the formation of the quasihexagonal overlayer structure coming from a two-dimensional condensation of adsorbed alkali-metal atoms and on the adsorbate-induced restructuring of the substrate surface including a missing-row type of restructuring. Recently, Fan and Ignatiev have thoroughly investigated the surface structures of Cs, or K formed on the Cu(110) surface with low-energy electron diffraction (LEED),² where they have revealed a variety of structures depending on coverage and temperature through the investigation of the phase transition and phase diagram for these systems. The structures have also been interpreted in terms of the quasihexagonal overlayer for those formed at low temperatures and the missing-row type of restructuring for those at elevated temperature.

On the other hand, according to a recent structural observation on Li/Cu(001), Tochihara and Mizuno³ have found anomalous LEED patterns assigned by (3×3) and (4×4) at final stages of Li deposition (0.4–0.7 monolayers) in their experiments on Li/Cu(001). For these two structures, they have suggested the presence of ordered surface alloys consisting of a two-dimensional Li-Cu compound formed on the substrate Cu(001) surface. The two structures followed the formation of the (2×1) structure which was determined recently by Mizuno, Tochihara, and Kawamura with LEED analysis to be a missing-row restructuring of the top layer of Cu(001).⁴ If the formation of surface alloys is true, the combination of

Li/Cu, where Li and Cu are the adsorbate and substrate, respectively, might be somewhat different in comparison with other combinations of other alkali-metal/Cu systems such as Cs/Cu,^{2,5} K/Cu,^{2,6} and Na/Cu,⁷ because simple overlayers or missing-row-type restructuring have been observed for the latter three systems at room temperature. The reason may come from the difference in the atomic size of alkali-metal adatoms. Consequently, a structural investigation of the Li/Cu(110) system is necessarily required as a next step, for further insight into the formation of surface alloys. Copel *et al.* have already studied the Li/Cu(110) system at room temperature by using LEED and ion scattering spectroscopy.⁸ They have observed a (1×2) LEED pattern and suggested the restructuring of the substrate Cu(110) surface. However, they did not observe any ordered structure other than the (1×2) structure with further increasing of Li coverage.

In this paper, we report the formation of a series of ordered structures at room temperature (300 K) following the (1×2) structure found by Copel *et al.*⁸ We propose that surface alloys similar to those observed on Cu(001) (Ref. 3) are also formed on the present Cu(110) surface. In addition, we show a variety of overlayer structures of Li formed on the Cu(110) surface at 90-K sample temperature.

II. EXPERIMENT

The experiments were carried out in an ultrahigh vacuum chamber equipped with a standard LEED optics capable of energy analysis for Auger electron spectroscopy (AES). The base pressure and the operating pressure during Li deposition were typically 3×10^{-11} and 1×10^{-10} Torr, respectively. The operating pressure was sufficient

to avoid contaminations during an experimental run of Li deposition. A commercial SAES getter source was employed for the Li evaporation source because of its simple handling. A Cu(110) sample with a size of $10 \times 15 \times 1$ mm was cut out of a large single crystal rod (40 mm diameter and 99.99% purity) and the orientation of the surface was confirmed by the x-ray Laue backscattering method to be less than 1° in accuracy with respect to the (110) crystallographic plane. A mirror finish of the sample surface was achieved in atmosphere by a combination of mechanical polishing with fine alumina powder and a chemical etching in an acid solution. An atomically clean surface was obtained by repeated cycles of the conventional Ar-ion sputtering (500 eV μ A) and annealing (770 K) procedures. The clean surface showed a well-defined LEED pattern of the (1×1) structure and non-detectable impurities in the AES spectra. The rate of Li deposition was typically 0.1 monolayer/min.

III. RESULTS

A. Auger uptake curve

A typical Auger spectrum from Li-deposited Cu(110) surfaces is shown in Fig. 1 with a spectrum from the clean surface. Two peaks at 46 and 50 eV were always observed for the Li-adsorbed surfaces. According to the previous work by Tochiyama and Mizuno on the Li/Cu(001) system,³ the 46-eV peak has been interpreted as coming from the Auger transition of $\text{Li}(1s)\text{Cu}(3d)\text{Cu}(3d)$ and the 50-eV peak from $\text{Li}(1s)\text{Li}(2s)\text{Li}(2s)$. Figures 2(a) and 2(b) show plots of the Auger intensity of the 46- and 50-eV peaks as a function of the deposition time at 90 and 300 K, respectively. The intensity of the 50-eV peak has deviated from the linear relationship, as seen in Fig. 2(a). From several experimental runs we can say that the deviation always appears at both temperatures. The nonlinearity indicates that the transition probability of this peak depends on the lateral arrangement of adsorbed Li atoms on Cu(110), because the electrons involved in the deexcitation process are valence electrons of Li adatoms.³ Details of the rela-

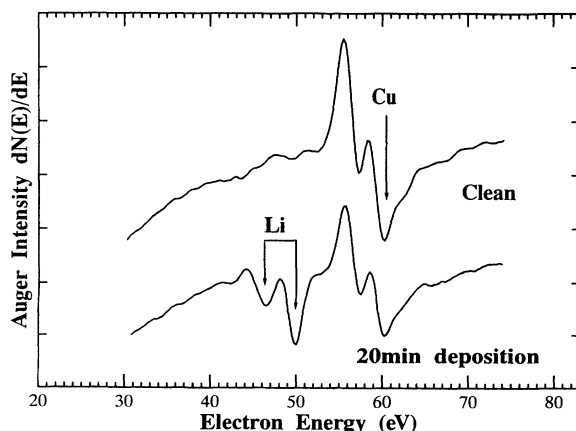


FIG. 1. Sample Auger spectra for (a) clean and (b) Li-deposited Cu(110) surface.

tion between the structure and the transition probability were not studied in this work. On the other hand, clearly the intensity of the 46-eV peak increases linearly with an increase of deposition at both temperatures. This behavior is consistent with the assignment of the transition of the 46-eV peak, because its intensity is expected to be proportional to the number of Li adatoms adsorbed on the bare Cu surface. Therefore, the 46-eV peak intensity was employed for the coverage estimation in this experiment under the reasonable calibration of the intensity described in Sec. III B 3.

There is a distinct difference in AES uptake curves between at 90 and 300 K, as seen in Fig. 2: At 90 K the intensity of the 46-eV peak stops increasing at the deposition time of 17 min, whereas at 300 K the intensity still increases after a break in slope at 15 min. The increase of the intensity after 15 min at 300 K was confirmed by a different experimental run. The dashed lines in Fig. 2(b) indicate the further increase of the AES intensities beyond the first breaks. The behavior is very similar to those observed for the Li/Cu(001) system.³ This difference between the two temperatures has been attributed to the different growth modes; at low temperatures Li overlayers are formed on Cu surfaces, while at room temperature intermixed layers of Li and Cu are formed.³ Therefore, the behaviors of the AES uptake curves suggest that similar growth modes are realized also for the present Li/Cu(110) system.

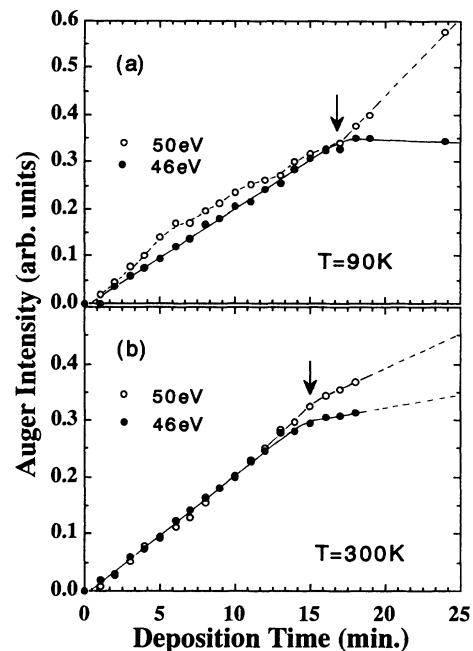


FIG. 2. Uptake curves of Auger intensity as a function of deposition time: (a) at 90 K and (b) at 300 K. Open and closed circles correspond to the Auger peaks of 50 and 46 eV, respectively. Arrows indicate break points corresponding to the completion of the first adsorbed layer. AES peak intensities were plotted after subtraction of the background slope using the data for the clean surface as a reference.

B. LEED observation

1. Li adsorption at 90 K

The deposition of Li onto Cu(110) at 90 K resulted in a sequence of changes in LEED pattern as shown in Fig. 3. The first superstructure observed is shown in Fig. 3(a), and its schematic LEED pattern is illustrated in Fig. 4. As seen in Fig. 4, all third-order spots exist in other incident energies. One may point out that only quasihexag-

onal spots (shown as ellipses in Fig. 4) are strong. If we choose the quasihexagonal spots as the unit cell for the superstructure, its coverage becomes too much greater than the estimated coverage which will be described in Sec. III B 3. Therefore, we concluded that the first superstructure is the (3×1) structure. Note that in this study we choose the $[\bar{1}10]$ direction as the $[10]$ direction of LEED patterns, as shown in Fig. 4. The next superstructure is shown in Fig. 3(b); its periodicity is denoted as (2×1) . From Fig. 3(c) it is found that the third structure

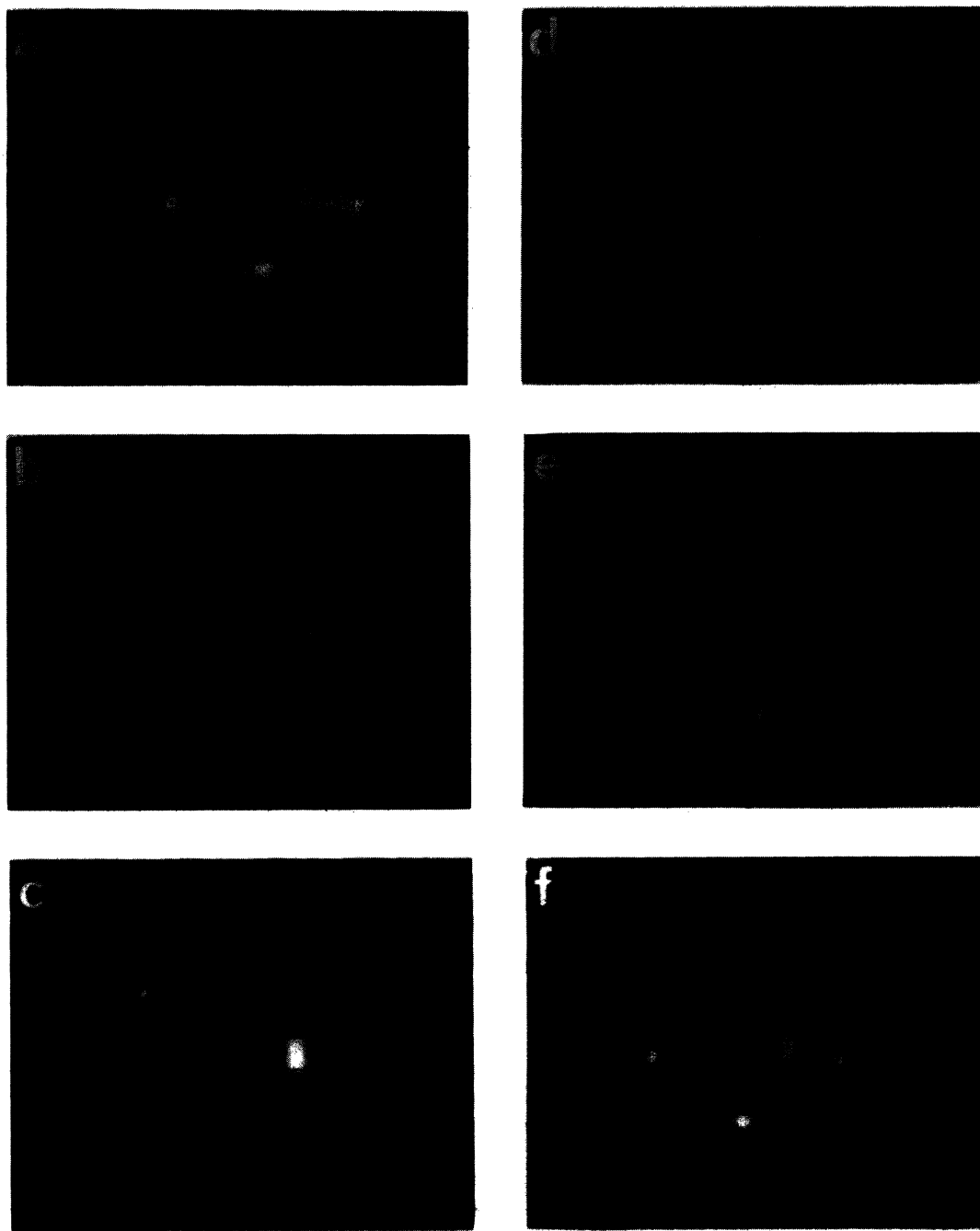


FIG. 3. LEED patterns of Li-covered structure on 90-K Cu(110) surface: (a) 3×1 at 138 eV; (b) 2×1 at 138 eV; and (c) 3×1 at 108 eV with weak 2×1 spots. The LEED patterns (d)–(f) were recorded at 138 eV and the structures are represented by a matrix notation denoted in the text.

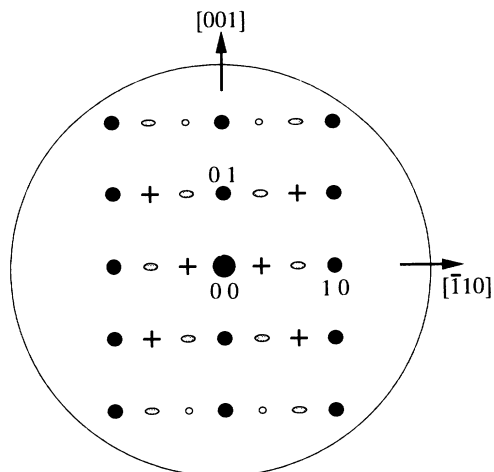


FIG. 4. Schematic illustration of the LEED pattern for Fig. 3(a). LEED spots represented by \circ and $+$ are very weak, but exist, and therefore the pattern is the (3×1) structure (see text).

is again (3×1) , although weak spots from the (2×1) structure remain there. Henceforth $(3 \times 1)''$ denotes the second (3×1) structure. The ratio of deposition times required to reach the best LEED patterns for each structure was 0.65:1.0:1.3 for the (3×1) , (2×1) , and $(3 \times 1)''$ structures, respectively. This ratio allows us to determine reasonable structure models for the three structures, as will be discussed in Sec. IV A.

Increasing Li deposition further, rather complicated LEED patterns appear as shown in Figs. 3(d)–3(f). The LEED patterns are somewhat mysterious. Streaky spots appeared around $\{7/10, 1/2\}$ and they seem to split as seen in Fig. 3(d), where the $(3 \times 1)''$ spots coexist. For convenience the LEED pattern around there is illustrated in Fig. 5. The split spots move towards the $\{1, 0\}$ or $\{1, 1\}$ spot with increasing Li coverage, as seen in Figs. 3(d)–3(f) and 5. The locus of the movement of the extra spot is represented by dotted lines in Fig. 5. A relevant unit cell for the extra spots is drawn for one domain. The extra spots seem to reach the $\{1, 0\}$ or $\{1, 1\}$ spot with increasing Li coverage as seen in Fig. 3(f). After the cover-

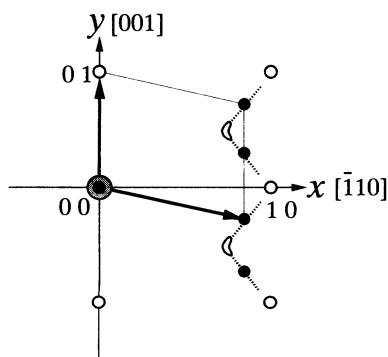


FIG. 5. Schematic illustration of LEED patterns for Figs. 3(d)–3(f). Segments terminated by an arrow indicate unit vectors in reciprocal space. A locus of the movement of the extra spot (closed circle) is depicted by a dotted line.

age corresponding to Fig. 3(f), however, the streaky spots disappeared and the LEED patterns look like the (1×1) structure with high background intensity.

2. Li adsorption at 300 K

Deposition of Li at 300 K resulted initially in streaks along the $[001]$ direction and subsequently in distinct half-order spots exhibiting the (1×2) structure, as shown in Fig. 6(b). The (1×2) structure was observed in a rather wide range of coverage. With further Li deposition, the (1×2) structure transformed to a disordered state (not shown in Fig. 6) with the (1×1) pattern accompanying a high background intensity. Then, a new series of superstructures was formed with the increase of deposition as shown in Figs. 6(c)–6(f); (4×1) , (5×1) , $(6 \times 1)^*$, and $(7 \times 1)^*$ structures, in which a complete set of fractional-order spots is found for each (4×1) and (5×1) pattern, while an incomplete set is found for the $(6 \times 1)^*$ or $(7 \times 1)^*$ pattern in which the separation between adjacent extra spots is not exactly $\frac{1}{6}$ or $\frac{1}{7}$ of that for normal spots. This means that the (4×1) and (5×1) structures are of perfect order and also commensurate with respect to the substrate surface, while the $(6 \times 1)^*$ and $(7 \times 1)^*$ structures are incomplete or consist of some mixture of $(n \times 1)$ domains with different n 's ($n=5-8$) but close to 6 or 7 in their average periodicity.

3. Li coverage

As already seen in Fig. 2, the first breaks in the slope of the AES uptake curves appeared at 17 and 15 min for 90 and 300 K, respectively. It is clear that these break points correspond to the completion of the first layer of Li on Cu(110). From AES, LEED, and comparison with the Li/Cu(001) system as described below, the break points were found to correspond to Li coverages of $\theta=1.0$ and 0.9 for 90 and 300 K, respectively, where the coverage θ means the fraction of density of Li adatoms with respect to the surface Cu density of Cu(110), i.e., $\theta=1$ corresponds to 1.1×10^{15} Li atoms/cm². The comparison of Li coverages on Cu(110) and Cu(001) was carried out by using the AES peak (46 eV) intensities, as mentioned below. It has already been determined that the Li coverage of the $c(2 \times 2)$ structure formed on Cu(001) at 180 K is 0.5 by LEED analysis.⁹ Therefore, we used the $c(2 \times 2)$ structure formed on Cu(001) as a standard number density of Li adatoms. From the comparison of the AES intensity of a well-defined (2×1) structure formed on Cu(110) at 90 K with that of the $c(2 \times 2)$ structure on Cu(001) in an experiment where both Cu(001) and Cu(110) specimens were set in the chamber, we concluded that the coverage for the (2×1) structure on Cu(110) is 0.5. We can estimate the Li coverage for other superstructures by using the AES peak intensity of Li (46 eV) calibrated by this standard. In Fig. 7, the superstructures observed in the present study are summarized as a function of Li coverage determined with the procedure above.

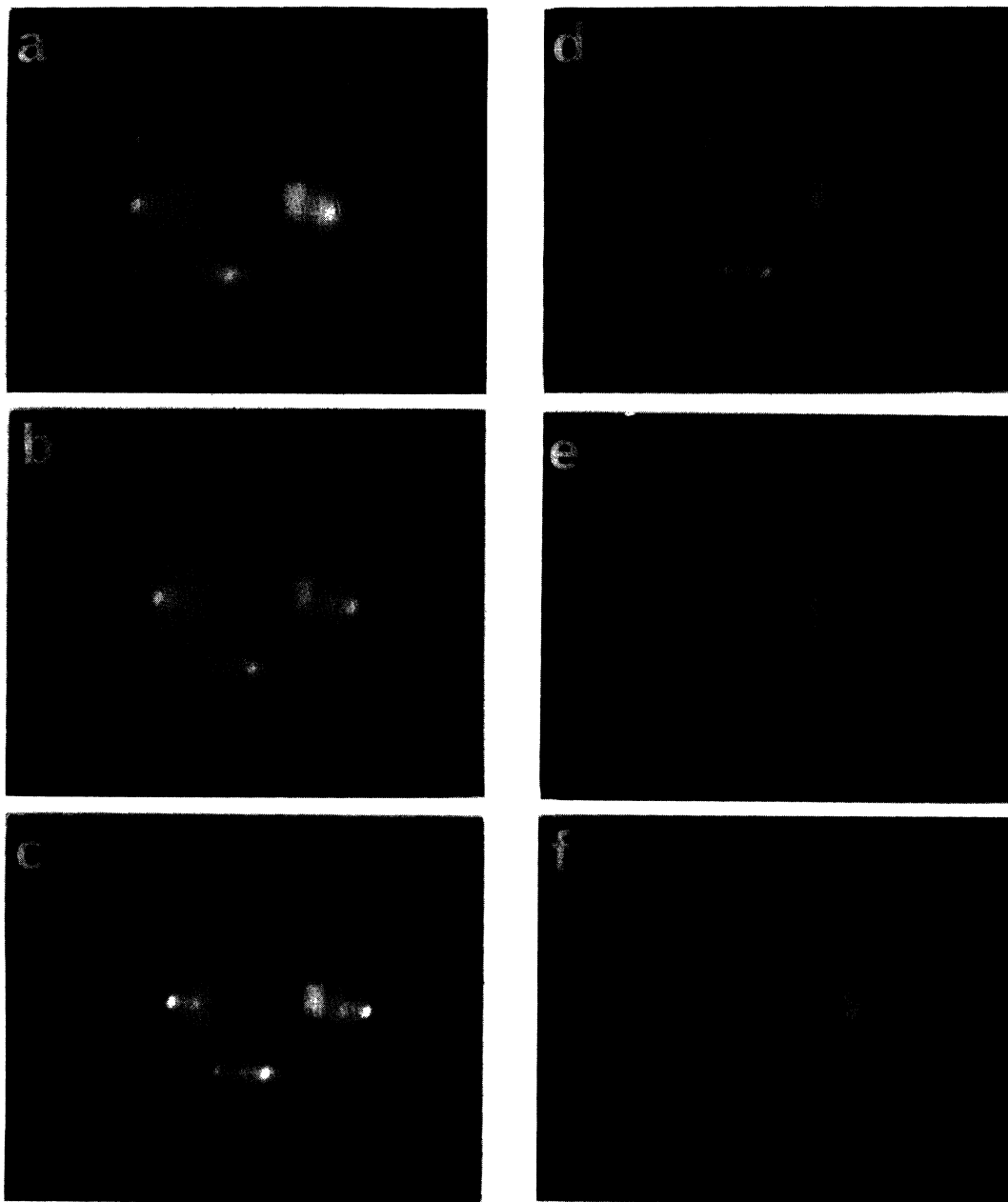


FIG. 6. LEED patterns of Li-covered structure observed on 300-K Cu(110) surface: (a) 1×1 at 142 eV; (b) 1×2 at 140 eV; (c) 4×1 at 138 eV; (d) 5×1 at 137 eV; (e) $n \times 1$ ($5 < n < 6$) at 109 eV; and (f) $n \times 1$ ($7 < n < 8$) at 109 eV.

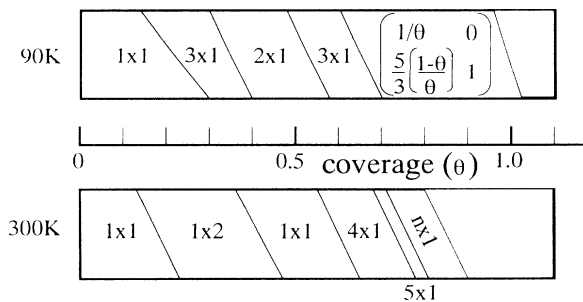


FIG. 7. Schematic illustration of the change of LEED pattern as a function of observed coverage.

IV. DISCUSSION

A. Models for superstructures formed at 90 K

Models for the superstructures formed at lower Li coverages at 90 K are shown in Figs. 8(a)–8(c), where all structures are assumed to be Li overlayers. Other possible structures would involve the restructuring of the substrate atoms. However, the temperature at which the substrate surface atoms start moving for restructuring has been known to be about 200 K for Cu(001).³ In addition, it is verified with LEED analysis that the $c(2 \times 2)$ structure formed on Cu(001) at 180 K is due to an overlayer of Li adatoms sitting on the hollow sites.⁹ There-

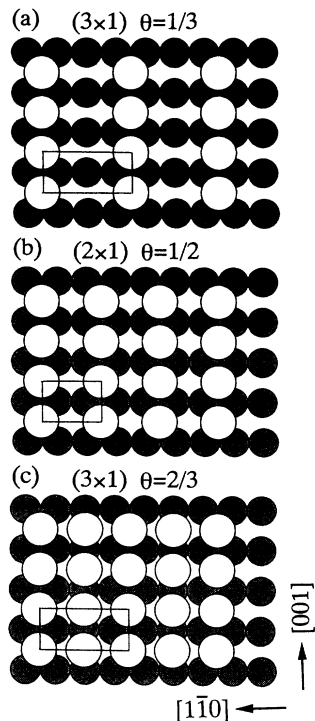


FIG. 8. Structure models for the 3×1 , 2×1 , and 3×1 LEED patterns in Figs. 3(a)–3(c). Open and gray closed circles denote Li and Cu atoms, respectively.

fore, the Li overlayer models are likely to be the case for the structures formed on Cu(110) at 90 K. We also assume that adsorbed Li atoms prefer to sit in the high coordination sites in the trough of the Cu(110) surface according to the previous reports,⁹ except for the $(3 \times 1)''$ structure where half of the Li adatoms inevitably reside on the longer bridge sites because of high coverage.

The proposed models [see Figs. 8(a)–8(c)] for the (3×1) , (2×1) , and $(3 \times 1)''$ structures are very simple. Li atoms appear to form one-dimensional chains along the $[001]$ direction, and the distance between adjacent chains regularly spaced is varied with increasing Li coverage. Coverages for the proposed models are obviously $\frac{1}{3}$, $\frac{1}{2}$, and $\frac{2}{3}$ for the (3×1) , (2×1) , and $(3 \times 1)''$ structures, leading to the coverage ratio of 0.67:1.0:1.33. This ratio well agrees with that of the deposition times described in Sec. III B 1. Therefore, the present models are most plausible and also this makes sure that the coverage of the (2×1) structure is 0.5, which gives a base of the calibration of the Auger peak intensity, as mentioned in Sec. III B 3.

So far, the adsorbate structure of one-dimensional chains has not been observed for alkali-metal adsorption on fcc(110) metals. Usually, quasihexagonal structures are formed, as reported for adsorption of K or Cs on Cu(110) at 80 K.² The formation of the quasihexagonal structures are considered to be due to a repulsive interaction between alkali-metal adatoms. The formation of one-dimensional chains in the present system suggests that there is an attractive interaction between adjacent Li adatoms along the $[001]$ direction, at least at low coverages such that Li adatoms occupy the hollow sites.

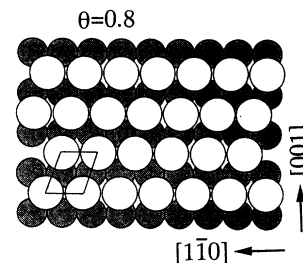


FIG. 9. A typical example of structure models for LEED patterns in Figs. 3(d)–3(f). The figure corresponds to the model for $\theta=0.8$; the oblique mesh (solid lines) indicates the unit cell of the surface structure formed by adsorbed Li atoms. Open and gray closed circles denote Li and Cu atoms, respectively.

Theoretical studies are required for understanding this new arrangement. We want to note that Li atoms can occupy the nearest neighbor sites along the $[001]$ direction on Cu(110), because the Li-Li distance (3.03 Å) of Li metal is smaller than the Cu-Cu distance (3.61 Å) along $[001]$. On the other hand, K or Cs atoms cannot make one-dimensional chains along $[001]$ because of their larger sizes.

Next we consider models for the superstructures formed at higher coverages of Li at 90 K [see Figs. 3(d)–3(f)]. As indicated in Fig. 5, the structural models should be consistent with the locus of the extra spots. Then the most reliable candidate of the structure model was found to be assigned by a matrix notation

$$\begin{pmatrix} \frac{1}{\theta} & 0 \\ \frac{5(1-\theta)}{3\theta} & 1 \end{pmatrix}$$

for the series of the LEED pattern in Figs. 3(d)–3(f), where $\theta > 0.7$. In this model, the position of the extra spot is denoted by $[\theta, \frac{5}{3}(\theta-1)]$ and then the locus of the spot $y = \frac{5}{3}(x-1)$, agrees well with the experimental result (see Fig. 5). A typical example of this model is shown in Fig. 9 for $\theta=0.8$. Basically, the atomic arrangement in this model is incommensurate with respect to that of the substrate along the $[1\bar{1}0]$ direction, and the character of the one-dimensional chains is broken. This suggests that the stability of the one-dimensional chains is ensured only under the condition of hollow-site occupation of Li adatoms.

B. Models for superstructures formed at 300 K

1. (1×2) structure

This structure is considered not to be a simple overlayer but to be due to restructuring of the substrate surface. The type of the restructuring was thought to be missing rows, in which every other close-packed row of the substrate surface atoms is lost. The deposited Li atoms are considered to exist in the trough of missing rows. For many combinations between alkali-metal and fcc(110) metal surfaces, the (1×2) structures have been observed since the first discovery by Hayden *et al.*¹⁰ The

(1×2) structure for the Li/Cu(110) system has already been observed by Copel *et al.*⁸ Nowadays, the (1×2) restructuring induced by alkali-metal adsorption of fcc(110) is established as missing-row structures by using ion scattering¹¹ and LEED analysis.^{12–14} Therefore, the (1×2) structure formed on Cu(110) by Li adsorption at 90 K in the present study is also considered to be caused by the missing-row type of restructuring of the substrate. As well as other systems, the (1×2) structure formed at 300 K did not transform to such structures as the (2×1) structure or others observed at 90 K, when the specimen temperature was cooled down to 90 K from 300 K. Conversely, the (1×2) structure was readily reproduced when the specimen was heated to 300 K after the appropriate deposition of Li at 90 K. This reflects that the (1×2) structure is formed through an irreversible activated process of the restructuring of the substrate surface atoms.

2. (4×1), (5×1), and (n×1) structures

To discuss the structure models for the LEED patterns observed at higher coverages at 90 K, it should be noticed that the structures (4×1), (5×1), and (n×1) were not observed at 90 K and, just as in the case of the (1×2) structure described above, the formation of these structure follows some irreversible activated process. Furthermore, it is interesting to note that the (4×1) structure followed a disordered state exhibiting the (1×1) LEED pattern. This suggests a start of another type of restructuring different from the missing row.

The most probable candidate of the structure model is a surface alloy of LiCu on Cu(110). From periodicities of (4×1) and (5×1) and their observed coverages, the structure models shown in Fig. 10(a) and 10(b), respectively, can be proposed. These structures consist of a regularly intermixed arrangement of Li and Cu atoms like a checkered pattern. The periodicity of the pattern changes along the [1 $\bar{1}$ 0] direction but not along the [001] direction with the increase of Li coverage. Proposed structures satisfy the following conditions required for these structural models. (i) The restructuring of the substrate surface atoms is different from the missing-row type. (ii) The coverage of Li should be in a range of 0.6–0.9 (see Fig. 7), and the coverage of the (4×1) structure is smaller than that of the (5×1) structure. (iii) Basically, structures of (4×1) and (5×1) should belong to the same category. Returning to the proposed models (see Fig. 10), we can make sure that these models satisfy the conditions above. For example, the coverages of the proposed models for the (4×1) and (5×1) structures are 0.75 and 0.8, respectively.

It is natural to consider that models of the (6×1)* and (7×1)* structures observed at higher coverages are similar to those of the (4×1) and (5×1) structures, the surface alloys. The structure model of the (7×1) shown in Fig. 10(c) instead of the (7×1)* for simplicity, because the observed (7×1)* structure may consist of some mixture of (n×1) domains with different n's (n=5–8) as described in Sec. III B 2. The coverage of the (7×1) structure is 0.86 and this value nicely follows 0.80 for the

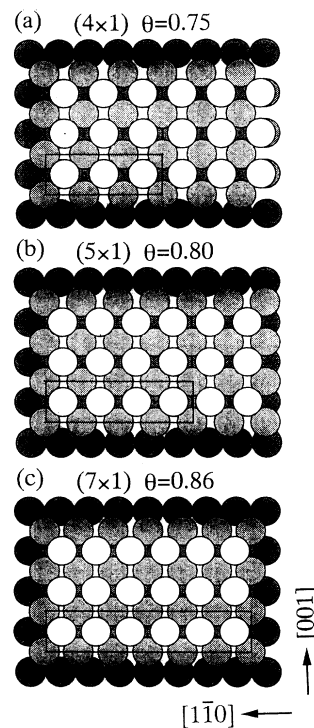


FIG. 10. Structure models for LEED patterns in Figs. 7(d)–7(f): the structure model (a) for 4×1 at $\theta=0.75$, (b) for 5×1 at $\theta=0.8$; and (c) for $n\times 1$ ($n=7$) at $\theta=0.86$. Dark and light gray circles correspond to Cu atoms, and open circles denote Li atoms.

(5×1) structure. With increasing Li coverage, the extra spots faded out and the LEED pattern exhibited the (1×1) structure with high background intensity.

Originally, the structure models of surface alloys have been proposed by Tochiara and Mizuno for the (3×3) and (4×4) structures formed on Cu(100) upon Li adsorption at 300 K.³ In this case, the isotropic nature of the (001) surface may lead to the formation of the isotropic surface-alloy layers. On the other hand, anisotropic superstructures such as (4×1) and (5×1) are formed on the Cu(110) surface in this study, which means that the unit vector of these surface alloys is the same as that of the substrate surface along the [001] direction and that this unit vector is fixed during formation of the (4×1), (5×1), and (n×1). This is interpreted in terms of the following assumption (i) and fact (ii). (i) The length of the unit vector of the two-dimensional alloy layer is essentially comparable to that of the substrate surface along the [001] direction. (ii) The amplitude of the periodic surface potential on the fcc(110) surface along the [001] direction is greater than that along the [1 $\bar{1}$ 0] direction. These two terms make the surface alloys be exactly commensurate with respect to the substrate surface along [001]. The assumption (i) is supported by the comparison with the Li/Cu(001) system as shown below. The lengths of the unit vectors of the two-dimensional alloy layers of the (3×3) and (4×4) structures on Cu(001) are $\frac{2}{3}a$ and $\frac{4}{3}a$, respectively, where a is the nearest-neighbor distance between Cu atoms along the close-packed row ($a=2.55$ Å).

That is, the length of the unit vector of the surface alloys along the [001] direction is $\sqrt{2}a$ for the Li/Cu(110) system, and this value is between $\frac{3}{2}a$ and $\frac{4}{3}a$, as mentioned above. Therefore, it is reasonable that the one unit vector always coincides with that of the Cu(110) surface along the [001] direction. Along the other direction, namely, $[\bar{1}\bar{1}0]$, the periodicity becomes 4, 5, and so on with increasing Li coverage, because the length of the unit vector of the surface alloy is much different from the length a of the substrate surface and the amplitude of the surface corrugation along $[\bar{1}\bar{1}0]$ is much smaller than that along [001]. These geometrical limitation leads the checkered pattern to multiple periodicities such as 4 and 5 or to be incommensurate along the $[\bar{1}\bar{1}0]$ direction.

Finally, we would like to emphasize that the checkered model of the surface alloy is believed to be common in the system of Li/Cu(hkl). The formation of the surface alloys is a matter of material synthesis on solid surfaces. Therefore, it is natural to consider that similar surface alloys are formed not only on (001) and (110) planes but also on other crystallographic planes. Of course, the structure of the surface alloys might be somewhat influenced by the structural symmetry of the substrate surfaces, as demonstrated in the present study. Further studies are very interesting and are in progress.

V. SUMMARY

We have observed coverage- and temperature-dependent surface structures formed on Cu(110) upon Li deposition by using LEED and AES of Li(KVV) transitions. For sample temperatures, we used 90 and 300 K as low and high temperatures. The observed superstructures are summarized in Fig. 7 as a function of Li coverage at two temperatures. At 90 K, the superstructures of (3×1) , (2×1) , and (3×1) are formed with increasing Li coverage up to 0.7. We have proposed that these structures consist of regularly spaced one-dimensional chains of Li adatoms along the [001] direction. For other alkali-metal adsorption, the chainlike structures have never been observed at low temperatures. The structures observed in a coverage range of 0.7–1.0 at 90 K are represented by a matrix notation

$$\begin{bmatrix} \frac{1}{\theta} & 0 \\ \frac{5(1-\theta)}{3\theta} & 1 \end{bmatrix},$$

where θ means the coverage of Li. In these structures the character of the one-dimensional chains are lost and Li adatoms form a oblique lattice sitting in troughs. All the structures developed at 90 K were assigned to be Li overlayers. The change of the structure depends simply on the balance between the adatom-adatom and adatom-substrate interactions.

At elevated temperature, 300 K, a missing-row-type restructuring with a (1×2) structure was observed at the coverage of around 0.3. Passing through a disordered surface structure at the coverages around $\theta=0.5$, other types of restructuring, considered to be a formation of surface alloys, were developed as a sequence of the LEED pattern, as seen in Fig. 7. These are the (4×1) , (5×1) , $(6 \times 1)^*$, and $(7 \times 1)^*$ structures, where the $(6 \times 1)^*$ and $(7 \times 1)^*$ structures are considered to be incomplete and may consist of some mixture of $(n \times 1)$ domains with different n 's ($n=5-8$). The proposed models for the (4×1) and (5×1) structure consist of regularly mixed arrangement of Li and Cu atoms such as the checkered pattern. These are ordered surface alloys of LiCu on Cu(110). The periodicity of the pattern changes along the $[\bar{1}\bar{1}0]$ direction but not along the [001] direction with the increase of Li coverage. The structure models for the surface alloys formed on Cu(110) are essentially the same as those of the (3×3) and (4×4) structures formed on Cu(100) with Li deposition at room temperature.³ This agreement suggests that the surface alloys of LiCu is generally formed on different crystallographic planes of copper single crystal, although the structures of the surface alloys might be modified by the symmetry of the substrates; the unit cells of the surface alloys on Cu(110) are rectangular, while those on Cu(001) are square.

ACKNOWLEDGMENTS

The authors would like to thank Dr. N. Fukuoka for his careful preparation of the copper sample. We also wish to thank Y. Narukawa for her great help with the experiments.

¹See, for example, *Physics and Chemistry of Alkali Metal Adsorption*, edited by H. P. Bonzel, A. M. Bradshaw, and G. Ertl (Elsevier, Amsterdam, 1989).

²W. C. Fan and A. Ignatiev, *Phys. Rev. B* **38**, 366 (1988).

³H. Tochiwara and S. Mizuno, *Surf. Sci.* **279**, 89 (1992).

⁴S. Mizuno, H. Tochiwara, and T. Kawamura, *Surf. Sci.* **292**, L811 (1993).

⁵J. Cousty, R. Riwan, and P. Soukiassian, *Surf. Sci.* **152/153**, 297 (1985).

⁶T. Argua, H. Tochiwara, and Y. Murata, *Surf. Sci.* **158**, 490 (1985).

⁷S. Mizuno and H. Tochiwara (unpublished).

⁸M. Copel, W. R. Graham, T. Custafsson, and S. Yalisove, *Solid State Commun.* **54**, 695 (1985).

⁹H. Tochiwara and S. Mizuno, *Surf. Sci.* **287/288**, 423 (1993); S. Mizuno, H. Tochiwara, and T. Kawamura, *ibid.* **293**, 239 (1993).

¹⁰B. E. Hayden, K. C. Prince, P. J. Davie, G. Paolucci, and A. M. Bradshaw, *Solid State Commun.* **54**, 325 (1983).

¹¹J. W. M. Franken, R. L. Kraus, J. F. van der Veen, E. Holub-Krappe, and K. Horn, *Phys. Rev. Lett.* **59**, 2307 (1987).

¹²C. J. Barnes, M. Q. Ding, M. Lindroos, D. J. Holmes, R. D. Diehl, and D. A. King, *Surf. Sci.* **162**, 59 (1985).

¹³C. J. Barnes, M. Lindroos, and D. A. King, *Surf. Sci.* **201**, 108 (1988).

¹⁴Z. P. Hu, B. C. Pan, W. C. Fan, and A. Ignatiev, *Phys. Rev. B* **41**, 9692 (1990).

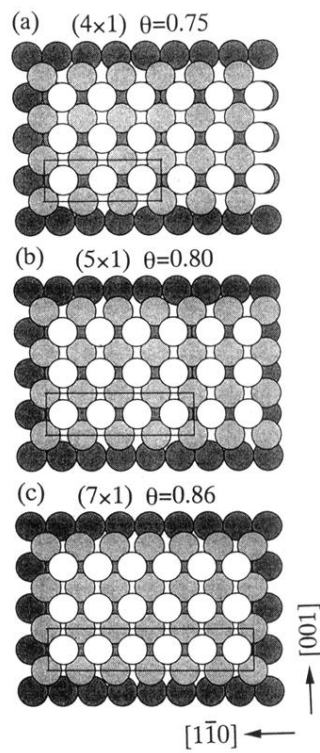


FIG. 10. Structure models for LEED patterns in Figs. 7(d)–7(f): the structure model (a) for 4×1 at $\theta=0.75$, (b) for 5×1 at $\theta=0.8$; and (c) for $n \times 1$ ($n=7$) at $\theta=0.86$. Dark and light gray circles correspond to Cu atoms, and open circles denote Li atoms.

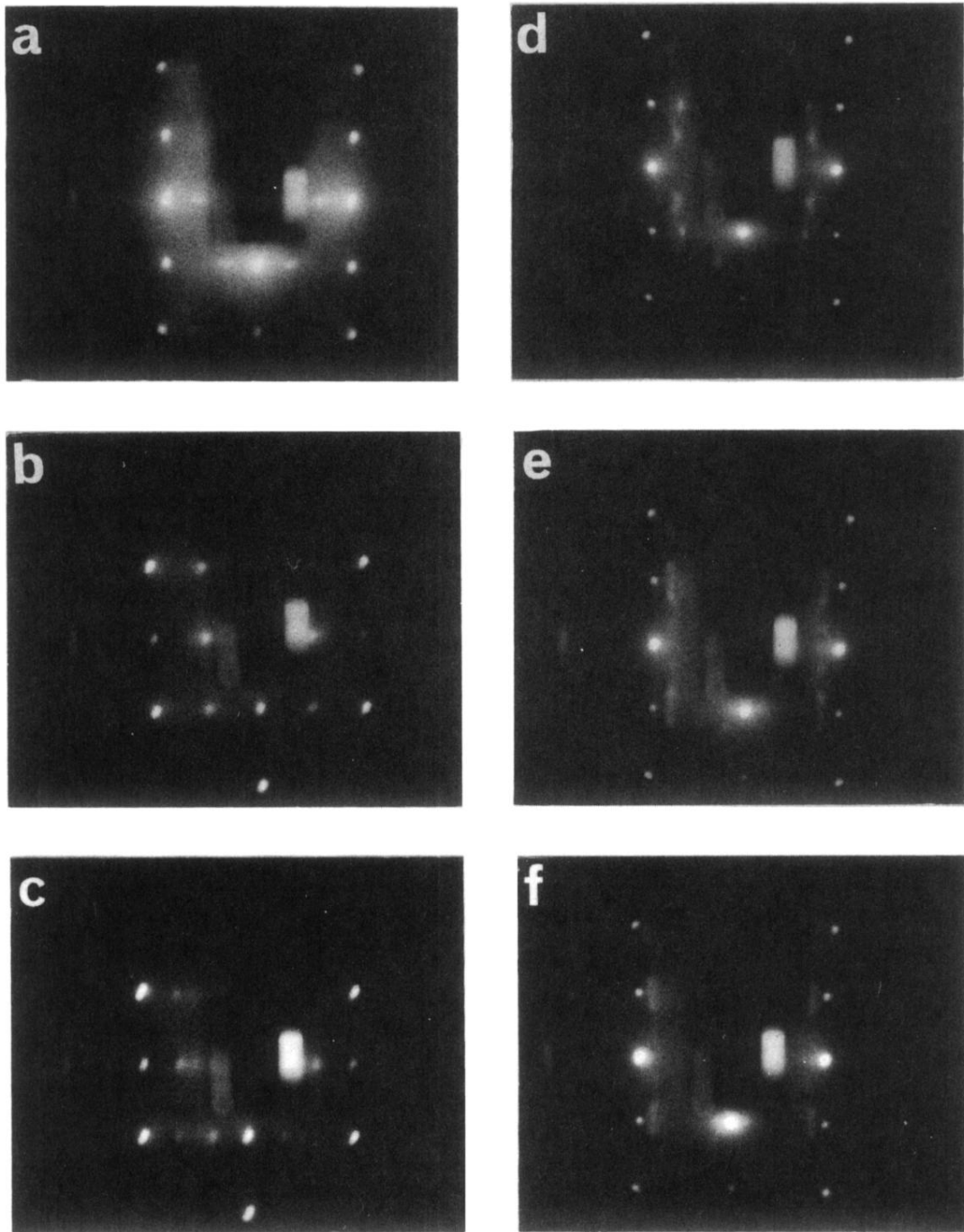


FIG. 3. LEED patterns of Li-covered structure on 90-K Cu(110) surface: (a) 3×1 at 138 eV; (b) 2×1 at 138 eV; and (c) 3×1 at 108 eV with weak 2×1 spots. The LEED patterns (d)–(f) were recorded at 138 eV and the structures are represented by a matrix notation denoted in the text.

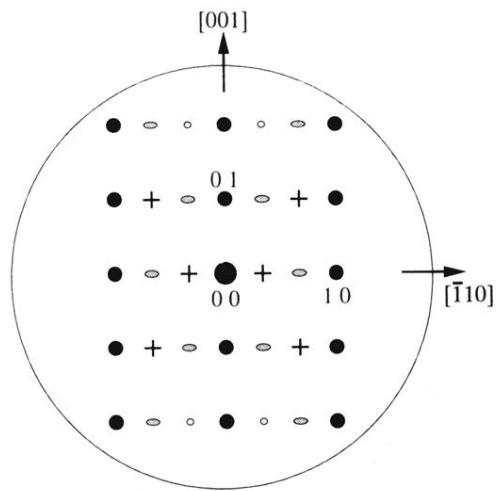


FIG. 4. Schematic illustration of the LEED pattern for Fig. 3(a). LEED spots represented by \circ and $+$ are very weak, but exist, and therefore the pattern is the (3×1) structure (see text).

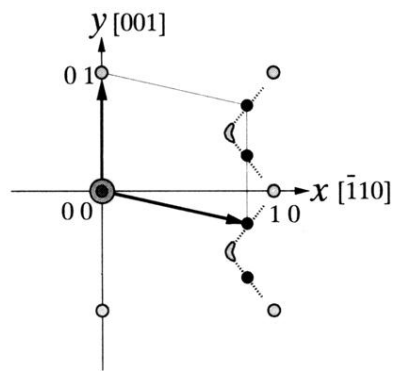


FIG. 5. Schematic illustration of LEED patterns for Figs. 3(d)–3(f). Segments terminated by an arrow indicate unit vectors in reciprocal space. A locus of the movement of the extra spot (closed circle) is depicted by a dotted line.

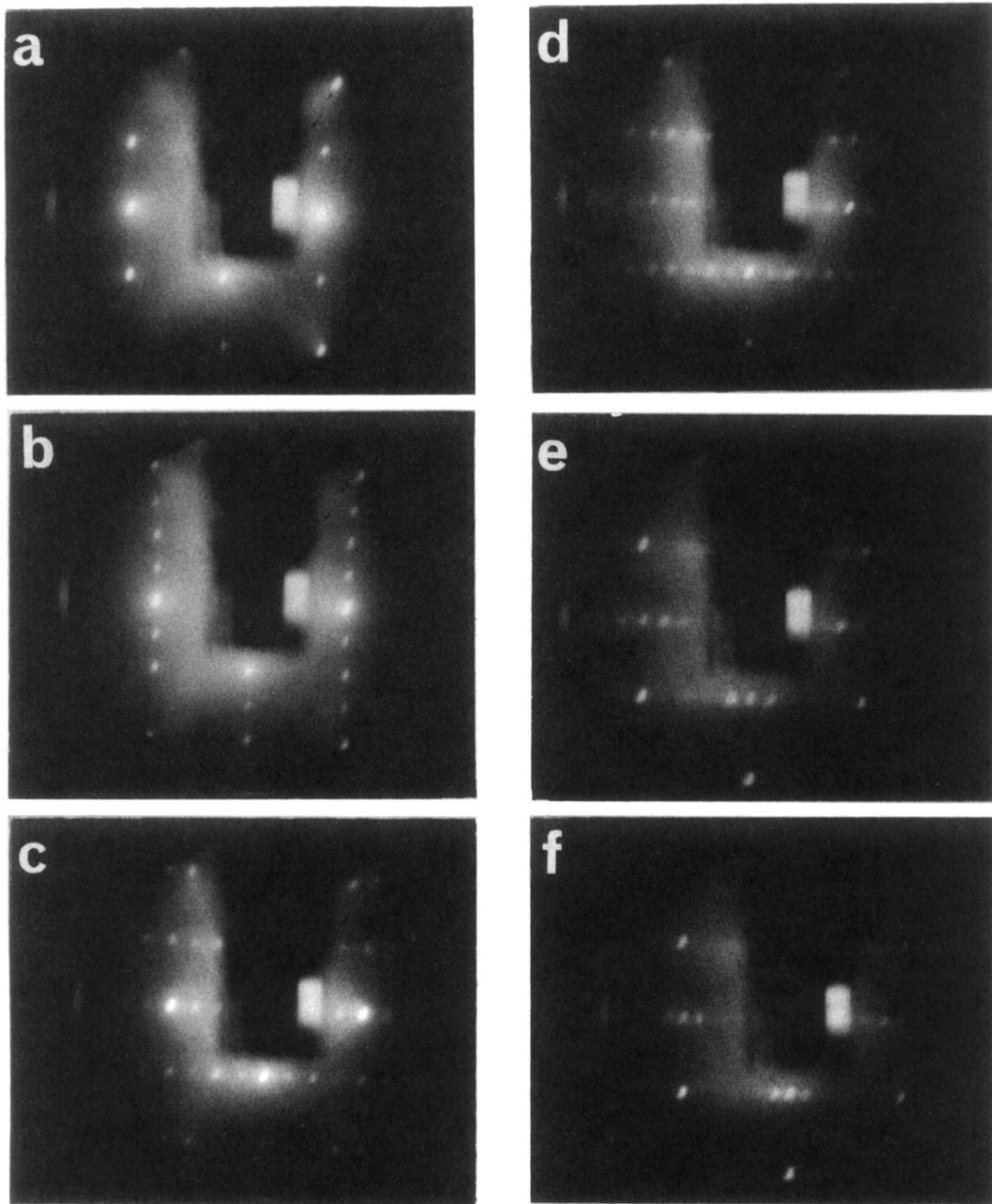


FIG. 6. LEED patterns of Li-covered structure observed on 300-K Cu(110) surface: (a) 1×1 at 142 eV; (b) 1×2 at 140 eV; (c) 4×1 at 138 eV; (d) 5×1 at 137 eV; (e) $n \times 1$ ($5 < n < 6$) at 109 eV; and (f) $n \times 1$ ($7 < n < 8$) at 109 eV.

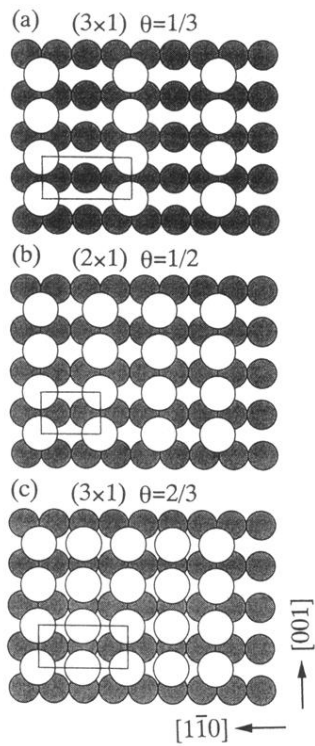


FIG. 8. Structure models for the 3×1 , 2×1 , and 3×1 LEED patterns in Figs. 3(a)–3(c). Open and gray closed circles denote Li and Cu atoms, respectively.

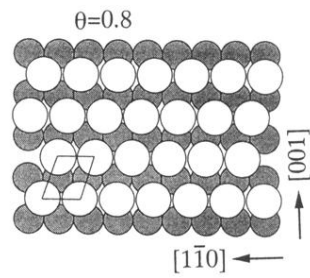


FIG. 9. A typical example of structure models for LEED patterns in Figs. 3(d)–3(f). The figure corresponds to the model for $\theta=0.8$; the oblique mesh (solid lines) indicates the unit cell of the surface structure formed by adsorbed Li atoms. Open and gray closed circles denote Li and Cu atoms, respectively.